Physics Letters A 384 (2020) 126835

Contents lists available at ScienceDirect

Physics Letters A

www.elsevier.com/locate/pla

The two-dimensional fractional discrete nonlinear Schrödinger equation

Mario I. Molina

Departamento de Física, Facultad de Ciencias, Universidad de Chile, Casilla 653, Santiago, Chile

ARTICLE INFO

Article history:
Received 2 July 2020
Received in revised form 18 August 2020
Accepted 19 August 2020
Available online 21 August 2020
Communicated by B. Malomed

Keywords:
Discrete nonlinear Schrodinger equation in 2D
Fractional Laplacian
Dispersion of linear modes
Nonlinear modes and stability
Selftrapping

ABSTRACT

We study a fractional version of the two-dimensional discrete nonlinear Schrödinger (DNLS) equation, where the usual discrete Laplacian is replaced by its fractional form that depends on a fractional exponent s that interpolates between the case of an identity operator ($s = 0$) and that of the usual discrete 2D Laplacian ($s = 1$). This replacement leads to a long-range coupling among sites that, at low values of s, decreases the bandwidth and leads to quasi-degenerate states. The mean square displacement of an initially-localized excitation is shown to be ballistic at all times with a 'speed' that increases monotonically with the fractional exponent s. We also compute the nonlinear modes and their stability for both, bulk and surface modes. The modulational stability is seen to increase with an increase in the fractional exponent. The trapping of an initially localized excitation shows a selftrapping transition as a function of nonlinearity strength, whose threshold increases with the value of s. In the linear limit, there persists a linear trapping at small s values. This behavior is connected with the decrease of the bandwidth and its associated increase in quasi-degeneracy.

Introduction. Let us consider the discrete nonlinear Schrödinger (DNLS) equation in d-dimensions [1–3]:

$$i\frac{dC_{\mathbf{n}}}{d\tau} + \sum_{\mathbf{m}} C_{\mathbf{m}} + \chi |C_{\mathbf{n}}|^2 C_{\mathbf{n}} = 0 \tag{1}$$

where the sum is over the nearest-neighbor sites. Parameters V and χ represent the coupling between nearest neighbor sites and the nonlinear coefficient, respectively. The DNLS equation has proven useful in describing a variety of phenomena in nonlinear Physics, such as propagation of excitations in a deformable medium [4,5], dynamics of Bose-Einstein condensates inside coupled magneto- optical traps [6,7], transversal propagation of light in waveguide arrays [8–11], self-focusing and collapse of Langmuir waves in plasma physics [12,13] and description of rogue waves in the ocean [14], among others. Its main features include the existence of localized nonlinear solutions with families of stable and unstable modes, the existence of a selftrapping transition [15,16] of an initially localized excitation, and a degree of excitation mobility in 1D [17]. All these characteristics have made the DNLS into a paradigmatic equation that describes the propagation of excitations in a nonlinear medium under a variety of different physical scenarios.

Recently, the topic of fractional derivatives has gained increased attention. It started with the observation that a usual integer-order derivative could be extended to a fractional-order derivative, that is, $(d^n/dx^n) \to (d^s/dx^s)$, for real s, which is known as the fractional exponent. The topic has a long history, dating back to letters exchanged between Leibnitz and L'Hopital, and later contributions by Euler, Laplace, Riemann, Liouville, and Caputo to name some. In the Riemann-Liouville formalism [18–20], the s-th derivative of a function $f(x)$ can be formally expressed as

$$\left(\frac{d^s}{dx^s}\right) f(x) = \frac{1}{\Gamma(1-s)} \frac{d}{dx} \int_0^x \frac{f(x')}{(x-x')^s} dx' \tag{2}$$

for $0 < s < 1$. For the case of the laplacian operator $\Delta = \partial^2/\partial \mathbf{r}^2$, its fractional form $(-\Delta)^s$ can be expressed as [21]

$$(-\Delta)^s f(\mathbf{x}) = L_{d,s} \int \frac{f(\mathbf{x}) - f(\mathbf{y})}{|\mathbf{x}-\mathbf{y}|^{d+2s}} \tag{3}$$

where,

$$L_{d,s} = \frac{4^s \Gamma[(d/2)+s]}{\pi^{d/2} |\Gamma(-s)|} \tag{4}$$

where $\Gamma(x)$ is the Gamma function, d is the dimension, and $0 < s < 1$ is the fractional exponent. Fractional order differential equations constitute useful tools to articulate complex events and to

E-mail address: mmolina@uchile.cl.

https://doi.org/10.1016/j.physleta.2020.126835
0375-9601/

model various physical phenomena. In particular, the fractional Laplacian (3) has found many applications in fields as diverse as fractional kinetics and anomalous diffusion [22–24], Levy processes in quantum mechanics [25], fluid mechanics [26,27], strange kinetics [28], fractional quantum mechanics [29,30], plasmas [31], biological invasions [32] and electrical propagation in cardiac tissue [33].

In this work we examine the consequences of replacing the usual two-dimensional discrete Laplacian by its fractional form, focusing on the effects on the existence and stability of nonlinear modes, as well as in the transport of excitations in a square lattice. In general, we find that the known DNLS phenomenology is more or less preserved, although there is a marked tendency towards band flattening as the fractional exponent s decreases. This causes an increase in the system's degeneracy and affects its capacity to selftrap excitations.

The model. For a square lattice ($d = 2$), the kinetic energy term $\sum_{\mathbf{m}} C_{\mathbf{m}}$ in Eq. (1), can be written as $4C_{\mathbf{n}} + \Delta_n C_{\mathbf{n}}$ where Δ_n is the discretized Laplacian

$$\Delta_n C_{\mathbf{n}} = C_{p+1,q} + C_{p-1,q} - 4\, C_{p,q} + C_{p,q+1} + C_{p,q-1}, \tag{5}$$

where $\mathbf{n} = (p, q)$. Equation (1) can then be written in dimensionless form as

$$i\frac{dC_{\mathbf{n}}}{dt} + 4C_{\mathbf{n}} + \Delta_n C_{\mathbf{n}} + \chi |C_{\mathbf{n}}|^2 C_{\mathbf{n}} = 0, \tag{6}$$

where $t \equiv V\tau$ and $\chi \equiv \gamma/V$. We proceed now to replace Δ_n by its fractional form $(\Delta_n)^s$ in Eq. (6). The form of this fractional discrete Laplacian for $d = 2$ is given by [35,36]

$$(\Delta_n)^s C_{\mathbf{n}} = \sum_{\mathbf{m}\neq\mathbf{n}} (C_{\mathbf{m}} - C_{\mathbf{n}})\; K^s(\mathbf{n} - \mathbf{m}) \tag{7}$$

where,

$$K^s(\mathbf{m}) = \frac{1}{|\Gamma(-s)|} \int_0^\infty e^{-4t}\; I_{m_1}(2t)\; I_{m_2}(2t)\; t^{-1-s}\, dt \tag{8}$$

with $\mathbf{m} = (m_1, m_2)$ and $I_m(x)$ is the modified special Bessel function. An alternative expression for $(\Delta_n)^s$ is

$$(\Delta_n)^s C_{\mathbf{j}} = L_{2,s} \sum_{\mathbf{m}\neq\mathbf{j}} (C_{\mathbf{m}} - C_{\mathbf{j}})\; G^{2,2}_{3,3}\left(\begin{matrix} 1/2, -(j2-m2+1+s, j2-m2+1+s) \\ 1/2+s, j1-m1, -(j1-m1) \end{matrix} \middle| 1 \right) \tag{9}$$

where $\mathbf{j} = (j_1, j_2)$ and $\mathbf{m} = (m_1, m_2)$, and $G(...)$ is the Meijer G-function. The symmetric kernel $K^s(\mathbf{m})$ plays the role of a long-ranged coupling. Near $s = 1$, $K(\mathbf{m}) \to \delta_{\mathbf{m},\mathbf{u}}$ where $\mathbf{u} = (1, 0)$ or $\mathbf{u} = (0, 1)$, i.e., coupling to nearest neighbors only. Let us look at its asymptotic form at long distances. Using

$$I_\nu(z) \sim \frac{1}{2\pi\nu}\left(\frac{ez}{2\nu}\right) \qquad \nu \to \infty, \tag{10}$$

plus $\Gamma(n) \sim n^{1/2}\; (n/e)^n$ and $\Gamma(n+s) \sim n^s\; \Gamma(n)$ for $n \to \infty$, one obtains

$$K^s(\mathbf{m}) \sim \left(\frac{m_1 + m_2}{m_1 m_2}\right) \frac{4^{-(m_1+m_2)}}{|\Gamma(-s)|} \frac{(m_1+m_2)^{m_1+m_2}}{m_1^{m_1} m_2^{m_2}} \tag{11}$$

where $\mathbf{m} = (m_1, m_2)$. Thus, for the 'diagonal' case $m_1 = m_2 = m$, one obtains

$$K^s(m) \sim \frac{1}{|\Gamma(-s)|} \frac{2^{-2m}}{\sqrt{m}} \qquad (m \to \infty). \tag{12}$$

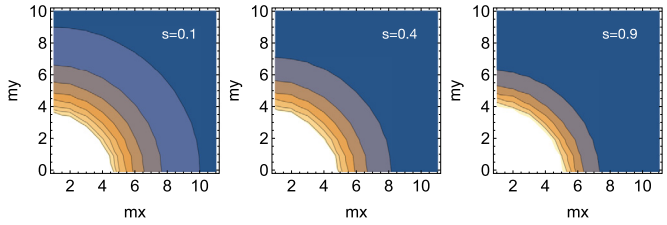

Fig. 1. Effective coupling $K(m_1, m_2)$ for several fractional exponents. $N = 11 \times 11$.

This decay is faster than in the one-dimensional case [34]. We consider now stationary modes defined by $C_{\mathbf{n}}(t) = e^{i\lambda t}\; \phi_{\mathbf{n}}$, which obey

$$(-\lambda + 4)\phi_{\mathbf{n}} + \sum_{\mathbf{m}\neq\mathbf{n}} (\phi_{\mathbf{m}} - \phi_{\mathbf{n}}) K^s(\mathbf{m} - \mathbf{n}) + \chi |\phi_{\mathbf{n}}|^2 \phi_{\mathbf{n}} = 0 \tag{13}$$

It should be mentioned that in expressions (6) and (13) the term 4 is to be replaced by 3 (2) for sites at the edge (corner), when dealing with a finite square lattice. Fig. 1 shows $K(\mathbf{m})$, where we see how the range of the coupling increases as s decrease. This has the effect of increasing the coupling between distant sites, leading to deep consequences, as we will show below.

Plane waves. Let us set $\chi = 0$ and look for plane wave solutions, $\phi_{\mathbf{n}} = A\;\; \exp(i\mathbf{k}.\mathbf{n})$, where we are assuming an infinite square lattice. After a short algebra, one obtains the dispersion relation,

$$\lambda(\mathbf{k}) = 4 + \sum_{\mathbf{m}} \left(e^{i\mathbf{k}.\mathbf{m}} - 1\right)\; K^s(\mathbf{m}) \tag{14}$$

Unfortunately, in this case it is not possible to rewrite Eq. (14) in closed form in terms of special functions, as in the one-dimensional case. Fig. 2 shows the bandwidth along two different directions in k-space. For both cases the bandwidth decreases monotonically as s decreases. This flattening of the band increases the degeneracy of the modes, and the system becomes closer to an ideal model known as the 'simplex' [37,38] where every site is coupled to every other site with equal strength. This leads to a strong localization of an initially localized excitation. In our case, this will become evident when we look at selftrapping.

Root mean square (RMS) displacement. One of the ways to quantify the propagation of an excitation across a lattice, is by the Root Mean Square (RMS) displacement, defined as

$$\langle \mathbf{n}^2 \rangle = \sum_{\mathbf{n}} \mathbf{n}^2\; |\phi_{\mathbf{n}}|^2 / \sum_{\mathbf{n}} |\phi_{\mathbf{n}}|^2. \tag{15}$$

A general result concerning RMS in lattices is that if $\lambda(-\mathbf{k}) = \lambda(\mathbf{k})$, $\lambda(\mathbf{k}) = \lambda(\mathbf{k} + 2\pi\mathbf{q})$ and $\nabla\lambda(\mathbf{k})|_{FBZ} = 0$, where FBZ is the first Brillouin zone, then it can be proven that the RMS for an initially localized excitation ($\phi_{\mathbf{n}}(0) = \delta_{\mathbf{n},\mathbf{0}}$) is always ballistic and given (in 2D) by [39]

$$\langle \mathbf{n}^2 \rangle = \left[\frac{1}{4\pi^2} \int_{\text{FBZ}} (\nabla\lambda(\mathbf{k}))^2\; d\,\mathbf{k} \right] t^2 \tag{16}$$

where FBZ is the first Brillouin zone. Using the form of $\lambda(\mathbf{k})$ given by Eq. (14), we obtain

$$\langle \mathbf{n}^2 \rangle = \sum_{\mathbf{m}} \mathbf{m}^2\; K^s(\mathbf{m}) K^s(-\mathbf{m}) \tag{17}$$

The parity properties of the modified Bessel functions, imply that $K^s(-\mathbf{m}) = K^s(\mathbf{m})$. Therefore,

$$\langle \mathbf{n}^2 \rangle = \left[\sum_{\mathbf{m}} \mathbf{m}^2 (K^s(\mathbf{m}))^2 \right] t^2 \tag{18}$$

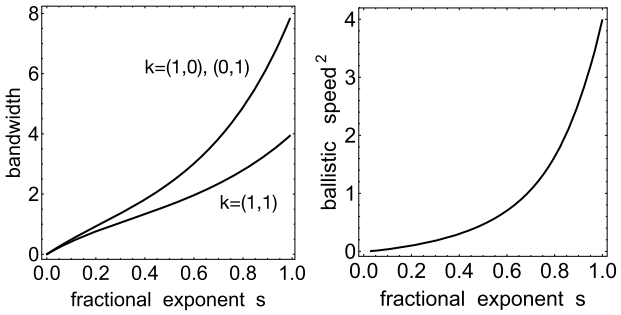

Fig. 2. Left: Bandwidth along three k-space directions, as a function of the fractional exponent s. Right: Characteristic ballistic speed (square) as a function of the fractional exponent. Note that as $s \to 1$, this speed approaches 2, as expected. ($N = 11 \times 11$).

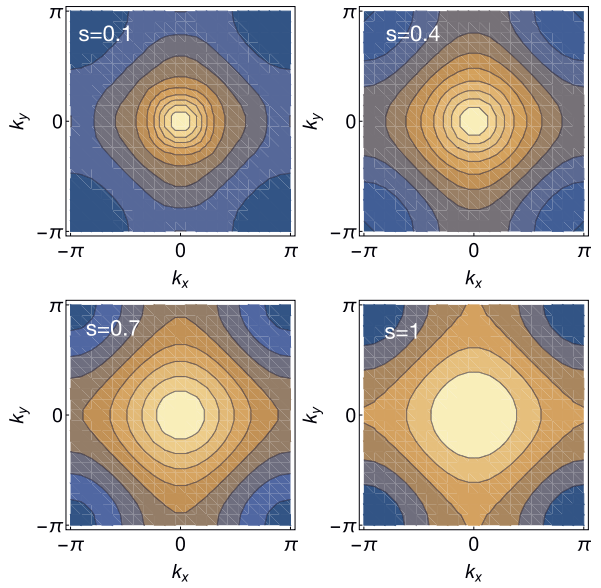

Fig. 3. Contour plot of $\lambda(k_x, k_y)$ for several fractional exponents. $N = 11 \times 11$.

where $\mathbf{m} = (m_1, m_2)$. The quantity inside the square brackets can be interpreted as the square of a characteristic ballistic speed. Given the rapid decrease of $K^s(\mathbf{m})$ with distance, $\langle \mathbf{n}^2 \rangle$ becomes well-defined for all $0 < s < 1$. Fig. 2b shows this speed square as a function of the fractional exponent s. The speed rises from zero at $s = 0$ up to 4 at $s = 1$, which is the usual ballistic value. The vanishing of the speed at $s = 0$ implies that, in this limit, the excitation is unable to move and remain localized at the initial site. In fact, at $s = 0$ any initial condition, which is a combination of all plane waves, will be unable to diffuse way. This result is in consonance with the observation that, at $s \to 0$, the band becomes completely degenerate, $\lambda(\mathbf{k}) \to 4$ causing the group velocity $\nabla\lambda(\mathbf{k})$ to vanish. In addition to the decrease in bandwidth, we also observe a steepening of the dispersion relation with a decrease in the fractional exponent, see Fig. 3.

Nonlinear modes. Let us consider now nonlinear modes ($\chi \neq 0$), i.e., solutions to Eqs. (13). They constitute a system of $N \times N$ nonlinear algebraic equations, where the form of the nonlinear term adopted here corresponds to Kerr nonlinearity found in coupled waveguide arrays, as well as in the semi classical description of an electron propagating in a deformable lattice. Numerical solutions are obtained by the use of a multidimensional Newton-Raphson scheme, using as a seed the solution obtained from the decoupled limit, also known as the anticontinuous limit. We take a finite $N \times N$ lattice with open boundary conditions and examine two-mode families, "bulk" modes, located far from the boundaries and "surface" modes located near the beginning (or end) of the lattice. The stability of these nonlinear modes is carried out in the standard manner, which we sketch here for completeness: We perturb our stationary solution $C_{\mathbf{n}}(t) = (\phi_{\mathbf{n}} + \delta_{\mathbf{n}}(t)) \exp(i\lambda t)$, where $|\delta_{\mathbf{n}}(t)| \ll |\phi_{\mathbf{n}}|$. We replace this in the evolution equation (6) [with $\Delta_{\mathbf{n}}$ replaced by $(\Delta_{\mathbf{n}})^s$]. After a linearization procedure, where we neglect any powers of $\delta_{\mathbf{n}}(t)$ beyond the linear one, we obtain a linear evolution equation for $\delta_{\mathbf{n}}(t)$. Next, we decompose $\delta_{\mathbf{n}}(t)$ into its real and imaginary parts: $\delta_{\mathbf{n}}(t) = x_{\mathbf{n}}(t) + i\ y_{\mathbf{n}}(t)$. To simplify the notation we map the sites of the two-dimensional square lattice into those of an open one-dimensional chain: $(n_1, n_2) \to n \equiv n_1 + (n_2 - 1)N$, with $1 \leq n_1, n_2 \leq N$. Then, the equations for $x_n(t)$ and $y_n(t)$ can be written in the form:

$$\frac{d^2}{dt^2}\,\vec{x} - \mathbf{A}\,\mathbf{B}\,\vec{x} = 0, \qquad \frac{d^2}{dt^2}\,\vec{y} - \mathbf{B}\,\mathbf{A}\,\vec{y} = 0, \tag{19}$$

where $\vec{x} = (x_1, x_2, \cdots x_{N\times N})$ and $\vec{y} = (y_1, y_2, \cdots y_{N\times N})$. Matrices $\mathbf{A}$ and $\mathbf{B}$ are given by

$$\mathbf{A}_{nm} = [-\lambda - K^s(0) + \epsilon_n + 2|\phi_n|^2 - \phi_n^2]\,\delta_{nm} + K^s(n-m) \tag{20}$$

$$\mathbf{B}_{nm} = [\lambda + K^s(0) - \epsilon_n - 2|\phi_n|^2 - \phi_n^2]\,\delta_{nm} - K^s(n-m) \tag{21}$$

where $\epsilon_n = \alpha - \sum_j K^s(n-j)$, with $\alpha = 2$ for a corner site, $\alpha = 3$ for an edge site, and $\alpha = 4$ for a bulk site. Linear stability is determined by the eigenvalue spectra of the matrices **AB** (or **BA**). When all eigenvalues are real and negative, the system is stable, otherwise it is unstable. In the more general case that considers possible complex eigenvalues, one defines the instability gain G as:

$$G = \text{Max of } \left\{ \frac{1}{2}\left(\text{Re}(g) + \sqrt{\text{Re}(g)^2 + \text{Im}(g)^2} \right) \right\}^{1/2} \tag{22}$$

for all g, where g is an eigenvalue of **AB** (**BA**). Thus, when $G = 0$, the mode under inspection is stable; otherwise it is unstable. Results from the above procedure are shown in Fig. 5 which shows power versus eigenvalue bifurcation diagrams for some bulk and surface modes, and for several values of the fractional exponents. Also shown are generic shapes of the two-dimensional modes. For these plots we have taken smaller lattices to reduce computation time. The modes span few sites only. This is due to our taking medium power levels. This is in order to display the effect of the fractional exponent on the shape of the modes. At smaller power levels, all modes would look bigger and more continuous but very similar to each other. An example of this can be seen in Fig. 4. Since we are dealing with a finite square lattice with open boundaries, there are two surface modes: the 'edge' one, and the 'corner' one. It is observed (not shown) that, after some few layers below the boundary, the surface modes become almost indistinguishable from the bulk ones. Thus, there is a continuous transition from surface to bulk modes. As for the bulk modes, we have focused on the 'odd' mode, centered on a single site, the 'even' mode, centered on two nearest-neighbor sites, and the 'ring' mode, centered around a closed loop of 4 sites (the two first names originate from the usage employed for one-dimensional lattices). For the bulk modes, we observe that the fundamental mode is always stable for all s values while the even and ring modes are unstable. All the bulk curves seem to touch the edge of the linear band, at low powers. As s is decreased, the modes become wider, but there are not other dramatic changes on the shape of the modes. The surface modes decay quickly away from the boundary, but their bifurcations curves look rather similar as s is varied.

An interesting special case to examine is that of the stability of a nonlinear uniform solution. In one-dimension, the instability of this mode has been observed to give rise to discrete

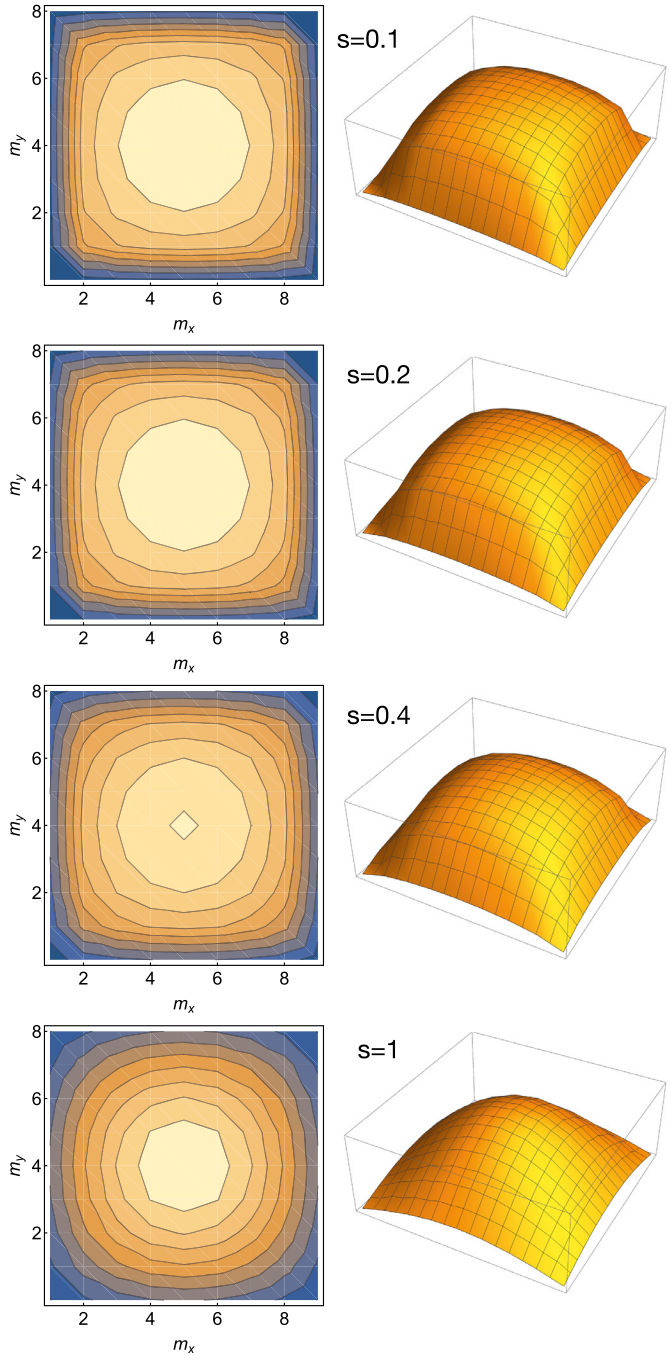

Fig. 4. Fundamental linear mode for several values of the fractional exponent. Left: Contour plots. Right: Three dimensional plots. $N = 11 \times 11$.

solitons and has, in fact, been proposed as a practical way to produce them [40]. Let us consider a solution of the form $C_{\mathbf{n}} = \phi\ \exp(i\lambda t)$. After replacing into the evolution equation one obtains $\lambda = 4 + \chi\phi^2$. Thus, $C_{\mathbf{n}}(t) = \phi\ \exp(i(4 + \chi\phi^2))$. After inserting this form into Eqs. (20) and (21), one obtains

$$\mathbf{A}_{nm} = [-\sum_{j\neq n} K^s(n-j)]\,\delta_{nm} + K^s(n-m) \tag{23}$$

$$\mathbf{B}_{nm} = [-\sum_{j\neq n} K^s(n-j) + 3\,\chi\,\phi^2]\,\delta_{nm} + K^s(n-m). \tag{24}$$

As before, we look at the eigenvalues of **AB** (or **BA**) and record the instability gain G. Fig. 6a shows G as a function of the nonlinearity strength, $\chi|\phi|^2$, for several fractional exponents. We notice

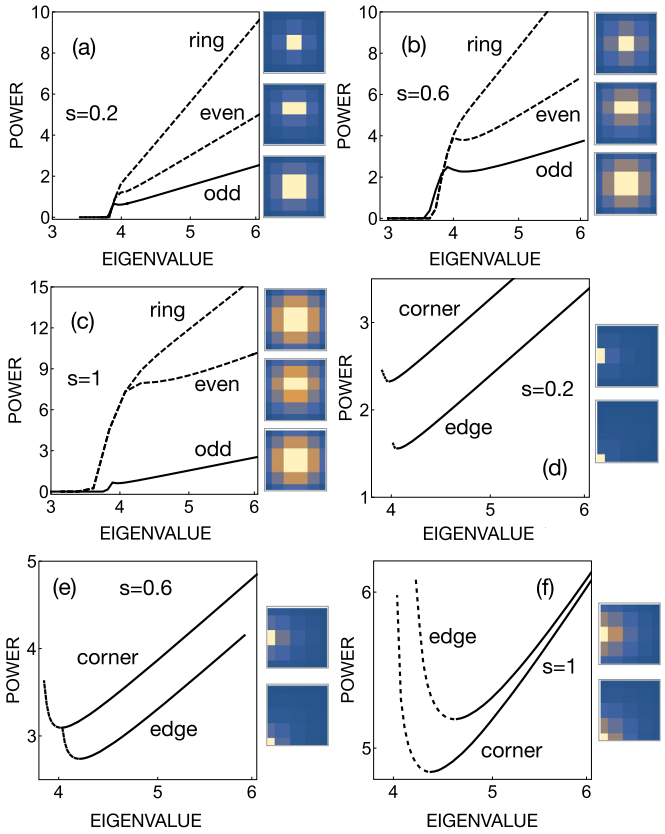

Fig. 5. Power content versus eigenvalue for some bulk and surface modes, for different fractional exponents. Continuous (dashed) curves denote stable (unstable) modes. $N = 5 \times 5$.

that, the stable region ($G = 0$) increases with an increase in the fractional exponent s. A possible explanation could be that, as s is decreased from a large value (i.e., near $s = 1$), the range of the coupling among sites increases, causing that any perturbation on a given site is instantly felt on distant sites. This situation of mutual, long-range perturbations inhibits the stability of the uniform front, as opposed that case when a perturbation of a given site only affects its immediate neighbors.

Selftrapping. One of the well-known effects of the Kerr nonlinearity is the onset of selftrapping where, for a nonlinearity strength above a threshold value, an initially localized excitation does not diffuse away completely when placed on a given site of the lattice. After some time, part of the excitation remains localized in the immediate vicinity of the initial site, while the rest diffuse away in a ballistic manner. We want to examine the possible effect of a fractional exponent on this trapping phenomenon. To ascertain the presence of a selftrapping transition, one examines the long-time average probability at the initial site (site 'zero')

$$\langle P_0\rangle = \frac{1}{T}\int_0^T |C_0(t)|^2\,dt \tag{25}$$

We have computed $\langle P_0\rangle$ for several s values, comparing the different selftrapping curves. Results are shown in Fig. 6b. We see that, as s is decreased from unity, the position of the selftrapping transition decreases as well and, in the linear limit we notice a degree of linear trapping that increases for lower values of s. These results can be explained as follows: as s is decreased, so does the width of the band (Fig. 2). This flattening of the bands originates a smaller group velocity of the modes. On the other hand, the local

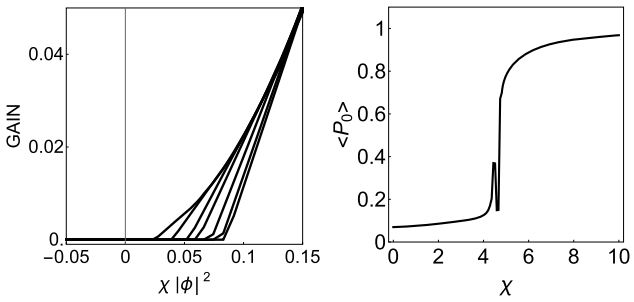

Fig. 6. Left: Modulational instability gain versus nonlinearity strength. From the leftmost to the rightmost curve $s = 0.1, 0.2, 0.4, 0.6, 0.8, 1.0$ ($N \times N = 25$). Right: Time-averaged probability at the initial site as a function of nonlinearity, for several different values of the fractional exponent, s. From the leftmost to the rightmost curve $s = 0.1, 0.2, 0.4, 0.6, 0.8$, and 1.0 ($T = 20, N \times N = 81$).

nonlinearity is roughly equivalent to a linear impurity of strength $\chi|\phi_0|^2$. Thus, we have an effective linear impurity embedded in a lattice whose modes have low group velocity (because of relatively flat band). The combination of these two effects, facilitates the trapping of the excitation and thus, decreases the nonlinearity threshold needed. There is yet another effect we can see in Fig. 6: As s decreases, the amount of trapping in the limit of zero nonlinearity increases. This linear trapping approaches unity for $s \to 0$ and is a consequence of the complete flattening of the band and a complete degeneracy of the modes. This special case has been examined before [37,38], with the result (adapted to our 2D case) that the time-averaged probability at the initial site is given by

$$\langle |C_0|^2 \rangle = \frac{(N \times N - 1)^2 + 1}{(N \times N)^2} \tag{26}$$

Therefore, at large N the trapped fraction approaches unity.

Conclusions. We have examined the consequences of employing a fractional version of the usual discrete Laplacian, parametrized by a fractional exponent, on the existence and stability of nonlinear modes, the free propagation of localized linear and nonlinear excitations, and the selftrapping of initially localized excitations, on a two-dimensional square lattice. We found that the main effect of a fractional exponent is to introduce a long-range coupling interaction among the sites of the lattice. The mean square displacement is always ballistic with a speed that decreases with a decrease in the fractional exponent. At small values of s, one observes a decrease in the bandwidth with a corresponding increase in degeneracy. The stability of the low-lying excitations is not dissimilar to the one found in the one-dimensional case, while the modulational stability increases with an increase in s. Finally, the selftrapping of an initially localized excitation shows a selftrapping transition with a threshold that increases with s, and shows a degree of linear selftrapping at low s values. This was explained to be a consequence of the increase in degeneracy as the band gets flatter and flatter as $s \to 0$.

The fact that the observed phenomenology observed for this two-dimensional system is not dissimilar to the one found for the one-dimensional analog, points out to the robustness of the discrete soliton phenomenology (nonlinear mode existence and stability, selftrapping, etc) not only against different parameter values of the DNLS equation, but against *different mathematical Laplacians*. Also, the fact that the effect of the fractional Laplacian is to introduce a long-range coupling means that one can reproduce experimentally the effect of a fractional Laplacian in an optical context, by setting up an appropriate distribution of refractive indices and inter site distances between waveguides in a waveguide array. Thus, it is possible in principle, to explore the fractional dynamics via optical experiments.

CRediT authorship contribution statement

M.I. Molina (the sole author) carried out all tasks associated with the creation of this paper, including conceptualization of original idea, methodology, theoretical calculations, numerical computations, writing of original and revised draft, funding acquisition.

Declaration of competing interest

The authors declare that they have no known competing financial interests or personal relationships that could have appeared to influence the work reported in this paper.

Acknowledgements

The author is grateful to Luz Roncal for valuable discussions. This work was supported by FONDECYT Grants 1160177 and 1200120.

References

[1] P.G. Kevrekidis, The Discrete Nonlinear Schrodinger Equation, Springer, Berlin Heidelberg, 2009.
[2] J.C. Eilbeck, P.S. Lomdahl, A.C. Scott, The discrete selftrapping equation, Physica D 16 (1985) 318–338.
[3] J.C. Eilbeck, M. Johansson, The discrete nonlinear Schrodinger equation-20 years on, in: Proceedings of the Conference on Localization and Energy Transfer in Non-linear Systems, Madrid, Spain, 2002, World Scientific, 2003.
[4] A.S. Davydov, Solitons and energy transfer along protein molecules, J. Theor. Biol. 66 (1977) 379–387.
[5] P.L. Christiansen, A.C. Scott (Eds.), Davydov's Soliton Revisited: Self-Trapping of Vibrational Energy in Protein, Plenum Press, New York, 1990.
[6] O. Morsh, M. Oberthaler, Dynamics of Bose-Einstein condensates in optical lattices, Rev. Mod. Phys. 78 (2006) 179–215.
[7] V.A. Brazhniy, V.V. Konotop, Theory of nonlinear matter waves in optical lattices, Mod. Phys. Lett. B 18 (2004) 627–651.
[8] D.N. Christodoulides, R.I. Joseph, Discrete self-focusing in nonlinear arrays of coupled waveguides, Opt. Lett. 13 (1988) 794–796.
[9] F. Lederer, G.I. Stegeman, D.N. Christodoulides, G. Assanto, M. Segev, Y. Silberberg, Discrete solitons in optics, Phys. Rep. 463 (2008) 1–126.
[10] Rodrigo A. Vicencio, Mario I. Molina, Yuri S. Kivshar, Phys. Rev. E 70 (2004) 026602.
[11] J.W. Fleischer, M. Segev, N.K. Efremidis, D.N. Christodoulides, Observation of two-dimensional discrete solitons in optically induced nonlinear photonic lattices, Nature 422 (2003) 147–150.
[12] V.E. Zakharov, Collapse and self-focusing of Langmuir waves, in: A.A. Galeev, R.N. Sudan (Eds.), Handbook of Plasma Physics, Vol. 2, Basic Plasma Physics, Elsevier North-Holland, 1984, pp. 81–121.
[13] V.E. Zakharov, Collapse of Langmuir waves, Sov. Phys. JETP 35 (1972) 908–914.
[14] M. Onorato, A.R. Osborne, M. Serio, S. Bertone, Freak waves in random oceanic sea states, Phys. Rev. Lett. 86 (2001) 5831.
[15] M.I. Molina, G.P. Tsironis, Dynamics of self-trapping in the discrete nonlinear Schrödinger equation, Physica D 65 (1993) 267–273.
[16] G.P. Tsironis, W.D. Deering, M.I. Molina, Applications of self-trapping in optically coupled devices, Physica D 68 (1993) 135–137.
[17] Rodrigo A. Vicencio, Mario I. Molina, Yuri S. Kivshar, Phys. Rev. E 70 (2004) 026602.
[18] R. Herrmann, Fractional Calculus - an Introduction for Physicists, World Scientific, Singapore, 2014.
[19] Bruce West, Mauro Bologna, Paolo Grigolini, Physics of Fractal Operators, Springer, 2003.
[20] Kenneth S. Miller, Bertram Ross (Eds.), An Introduction to the Fractional Calculus and Fractional Differential Equations, John Wiley & Sons, 1993.
[21] N.S. Landkof, Foundations of Modern Potential Theory (translated from the Russian by A.P. Doohovskoy), Die Grundlehren der Mathematischen Wissenschaften, vol. 180, Springer-Verlag, New York, 1972.
[22] R. Metzler, J. Klafter, The random walk's guide to anomalous diffusion: a fractional dynamics approach, Phys. Rep. 339 (2000) 1–77.
[23] I.M. Sokolov, J. Klafter, A. Blumen, Fractional kinetics, Phys. Today 55 (2002) 44–58.
[24] G.M. Zaslavsky, Chaos, fractional kinetics, and anomalous transport, Phys. Rep. 371 (2002) 461–580.
[25] N.C. Petroni, M. Pusterla, Levy processes and Schrodinger equation, Physica A 388 (2009) 824.
[26] L.A. Caffarelli, A. Vasseur, Drift diffusion equations with fractional diffusion and the quasi-geostrophic equation, Ann. Math. 171 (2010) 1903–1930.

[27] P. Constantin, M. Ignatova, Critical SQG in bounded domains, Ann. PDE 2 (2016) 1–42.
[28] M.F. Shlesinger, G.M. Zaslavsky, J. Klafter, Strange kinetics, Nature 363 (1993) 31–37.
[29] N. Laskin, Fractional quantum mechanics, Phys. Rev. E 62 (2000) 3135.
[30] N. Laskin, Fractional Schrodinger equation, Phys. Rev. E 66 (2002) 056108.
[31] M. Allen, A fractional free boundary problem related to a plasma problem, Commun. Anal. Geom. 27 (2019) 1665.
[32] H. Berestycki, J.-M. Roquejoffre, L. Rossi, The influence of a line with fast diffusion on Fisher-KPP propagation, J. Math. Biol. 66 (2013) 743.
[33] A. Bueno-Orovio, D. Kay, V. Grau, B. Rodriguez, K. Burrage, Fractional diffusion models of cardiac electrical propagation: role of structural heterogeneity in dispersion of repolarization, J. R. Soc. Interface 11 (97) (2014) 20140352.
[34] M.I. Molina, The fractional discrete nonlinear Schrödinger equation, Phys. Lett. A 384 (2020) 126180.
[35] Oscar Ciaurri, Luz Roncal, Pablo Raul Stinga, Jose L. Torrea, Juan Luis Varona, Nonlocal discrete diffusion equations and the fractional discrete Laplacian, regularity and applications, Adv. Math. 330 (2018) 688.
[36] Luz Roncal, private communication.
[37] Danilo Rivas, Mario I. Molina, Selftrapping in flat band lattices with nonlinear disorder, Sci. Rep. 10 (2020) 5229.
[38] J.D. Andersen, V.M. Kenkre, Self-trapping and time evolution in some spatially extended quantum nonlinear systems: exact solutions, Phys. Rev. B 47 (1993) 11134.
[39] A.J. Martinez, M.I. Molina, Diffusion in infinite and semi-infinite lattices with long-range coupling, J. Phys. A, Math. Theor. 45 (2012) 275204.
[40] Y.S. Kivshar, M. Peyrard, Modulational instabilities in discrete lattices, Phys. Rev. A 46 (1992) 3198.